Mathematical and Computational Applications

MDPI

Article

Modeling the Impact of Treatment Adherence on Hepatitis C Transmission Dynamics Among Intravenous Drug Users

Mlyashimbi Helikumi [1], Tinashe Victor Mupedza [2], Shingirai Tangakugara Murambiwa [2], Moster Zhangazha [3] and Adquate Mhlanga [4,*]

[1] Department of Mathematics and Statistics, College of Science and Technical Education, Mbeya University of Science and Technology, Mbeya P.O. Box 131, Tanzania
[2] Department of Mathematics, University of Zimbabwe, Harare P.O. Box MP 167, Zimbabwe
[3] Department of Mathematics and Applied Mathematics, University of Johannesburg, Johannesburg 2006, South Africa
[4] The Program for Experimental and Theoretical Modeling, Division of Hepatology, Department of Medicine, Stritch School of Medicine, Loyola University Chicago, Maywood, IL 84101, USA
* Correspondence: ngoni72@gmail.com or amhlanga@luc.edu

Abstract

Hepatitis C virus (HCV) infection remains highly prevalent among people who inject drugs (PWID), where treatment effectiveness is strongly influenced by adherence and behavioral relapse. In this study, we develop and analyze a deterministic compartmental model to examine the impact of treatment adherence, relapse, and risk-reduction behaviors on HCV transmission dynamics. The model incorporates key behavioral pathways, including treatment initiation, partial adherence, and relapse to high-risk behavior. Analytical results establish positivity and boundedness of solutions, and the basic reproduction number is derived using the next-generation matrix approach. We show that the disease-free equilibrium is globally asymptotically stable when the reproduction number is below unity, while uniform persistence and a globally stable endemic equilibrium occur when transmission exceeds this threshold. Numerical simulations and sensitivity analyses indicate that the probability of transmission per needle-sharing event and the number of sharing partners are dominant drivers of epidemic persistence. In contrast, treatment uptake and sustained adherence significantly reduce transmission. Relapse to drug misuse undermines treatment benefits by expanding the infectious pool. These findings underscore the importance of integrating antiviral therapy with behavioral support to achieve long-term HCV control among PWID.

Keywords: hepatitis C virus; intravenous drug users; treatment adherence; mathematical modeling; basic reproduction number

Check for updates

Academic Editor: Gianluigi Rozza

Received: 25 July 2026
Revised: 26 August 2026
Accepted: 26 August 2026
Published: 1 September 2026

Copyright: © 2026 by the authors. Licensee MDPI, Basel, Switzerland. This article is an open access article distributed under the terms and conditions of the Creative Commons Attribution (CC BY) license.

1. Introduction

Hepatitis C virus (HCV) infection is believed to have originated approximately 500–2000 years ago, as inferred from analyses of its molecular diversity and evolutionary history [1]. Today, HCV is recognized as a major global burden of disease [2]. Epidemiological studies have estimated that roughly 180 million people worldwide have been infected with HCV, and the virus remains a leading cause of chronic liver disease, liver-related mortality, and liver transplantation in several countries [3–5]. Projections have further suggested that HCV-related mortality, primarily due to liver failure and hepatocellular carcinoma, would continue to rise over subsequent decades in the absence of effective control

strategies [3–5]. Over the past three decades, HCV has therefore emerged and persisted as a major global public health concern. More recently, the World Health Organization (WHO) estimated that in 2019 approximately 58 million people were living with chronic HCV infection worldwide, with about 1.5 million (1.3–1.8 million) new infections and 290,000 deaths attributable to HCV-related complications [6]. This represented a reduction of approximately 6.8 million viremic infections compared with the estimated 63.6 million cases in 2015, largely reflecting the widespread introduction and scale-up of direct-acting antiviral (DAA) therapies [6].

HCV is a blood-borne virus transmitted through exposure to infected blood, most commonly via injection drug use, contaminated blood transfusions, vertical (mother-to-child) transmission, organ transplantation, or sexual contact [7]. Clinical symptoms may take decades to appear, and as a result nearly half of individuals living with HCV are unaware of their infection. The incubation period for HCV ranges from approximately two weeks to six months [8]. These prolonged asymptomatic periods complicate surveillance and are relevant for assessing changes in disease incidence, particularly when susceptibility and infectiousness vary within populations [9]. In most developed countries and many developing settings, people who inject drugs (PWID) remain the primary risk group for HCV infection and therefore represent a key priority for prevention interventions [10]. The burden of HCV among PWID is especially high, with an estimated 52% having evidence of past or current HCV infection globally [11]. Consequently, achieving the WHO targets for HCV elimination will require sustained and targeted efforts to reduce transmission within this population. Despite major advances in HCV treatment, including DAAs and host-targeting agents (HTAs), a universally effective therapy remains elusive. Earlier standard treatment with pegylated interferon (IFN) was characterized by limited efficacy and substantial adverse effects [12], and to date no prophylactic vaccine against HCV is available.

Infectious disease transmission models have been widely used to predict the magnitude and duration of outbreaks, estimate key biological and clinical parameters, and evaluate the potential impact of intervention strategies [13,14]. The structure of a transmission model is typically guided by the specific scientific or public health question being addressed and tailored to the pathogen of interest, allowing it to provide powerful insights into the mechanisms driving disease dynamics [15]. Such models also offer a flexible quantitative framework for systematically exploring the effectiveness of a wide range of mitigation and control approaches [14].

Several mathematical models have been developed to investigate HCV transmission among people who inject drugs, considering different aspects of interventions [16–25]. In particular, Mushayabasa and Bhunu [25] investigated the impact of antiviral therapy, abstinence and relapse on the transmission dynamics of HCV epidemics among intravenous drug misusers. Building on these previous studies, the present work further examines how treatment engagement and adherence-related behavioral changes influence HCV transmission and persistence. We further investigate the relative influence of these treatment and behavioral factors on the basic reproduction number, R_0, and identify conditions under which HCV transmission can persist or be controlled. Thus, this study provides additional insight into the combined role of treatment adherence, behavioral change, and relapse in HCV transmission among people who inject drugs.

The remainder of this paper is organized as follows. Section 2 presents the formulation of the mathematical model describing hepatitis C transmission dynamics among people who inject drugs. Section 3 is devoted to the model analysis. Section 4 provides a discussion of the results and concluding remarks.

2. Model Formulation

Based on the epidemiological status, the total population of intravenous drug misusers, denoted by N, is divided into five epidemiological classes: susceptible individuals (S), infectious individuals not on treatment (I), infectious individuals on treatment who have abstained from drug misuse activities (T), infectious individuals on treatment who remain active in intravenous drug misuse but have reduced their number of needle-sharing partners (H), and recovered individuals (R). The compartmental structure and transitions among these epidemiological classes are illustrated in Figure 1. Thus, $N = S + I + T + H + R$. Intravenous drug misusers on HCV treatment are encouraged to abstain from drug misuse activities; however, some fail to adhere due to factors such as addiction and peer influence. Others respond by reducing their partner acquisition rate. Susceptible individuals acquire HCV infection by sharing contaminated needles or syringes at a rate

$$\lambda = \frac{(1-\delta)\beta(cI + \phi(1-\eta)H)}{N},$$

where β represents the probability of HCV transmission per needle-sharing event, c is the average number of needle-sharing partners for individuals in class I, ϕ ($\phi < c$) is the partner acquisition rate for individuals in class H, η is a parameter accounting for the reduced likelihood of HCV transmission by individuals in class H, and δ is the proportion of acute infections that clear spontaneously. A similar force of infection has been applied before; see [22]. Infectious individuals in class I seek treatment at a rate ρ, after which a proportion α abstains from drug misuse and transitions to class T, while the remaining proportion $(1-\alpha)$ reduces their risky behaviors and moves to class H. After successful treatment, individuals in class H and those in class T recover at rates ω_1 and ω_2, respectively. Natural mortality, assumed to be constant across all classes, occurs at rate μ. Due to drug addiction, individuals in class T may relapse to drug misuse activities at a rate θ, with a proportion r returning to high-risk behavior (I) and the remaining proportion $(1-r)$ transitioning to reduced-risk behavior (H). Furthermore, individuals in class H may deteriorate in behavioral control and move to the high-risk infectious class I at the same rate θ, reflecting the assumption that both treated groups are subject to similar addiction-driven instability, although their post-transition behaviors differ. The parameter θ therefore represents a general rate of treatment-related behavioral deterioration affecting both T and H, while heterogeneity in post-transition outcomes is captured by the parameter r. Assuming homogeneous mixing and constant recruitment of new intravenous drug misusers into the susceptible class at rate Λ, these dynamics are described by a system of nonlinear differential equations that govern the interactions between treatment, infection, and behavior among intravenous drug misusers.

The system of nonlinear differential equations governing the model is given by:

$$\begin{aligned}
\frac{dS}{dt} &= \Lambda - \frac{(1-\delta)\beta(cI + \phi(1-\eta)H)S}{N} - \mu S,\\
\frac{dI}{dt} &= \frac{(1-\delta)\beta(cI + \phi(1-\eta)H)S}{N} + \theta(rT + H) - (\rho + \mu)I,\\
\frac{dH}{dt} &= (1-r)\theta T + (1-\alpha)\rho I - (\mu + \omega_1 + \theta)H,\\
\frac{dT}{dt} &= \alpha\rho I - (\mu + \omega_2 + \theta)T,\\
\frac{dR}{dt} &= \omega_1 H + \omega_2 T - \mu R.
\end{aligned} \tag{1}$$

https://doi.org/10.3390/mca31050176

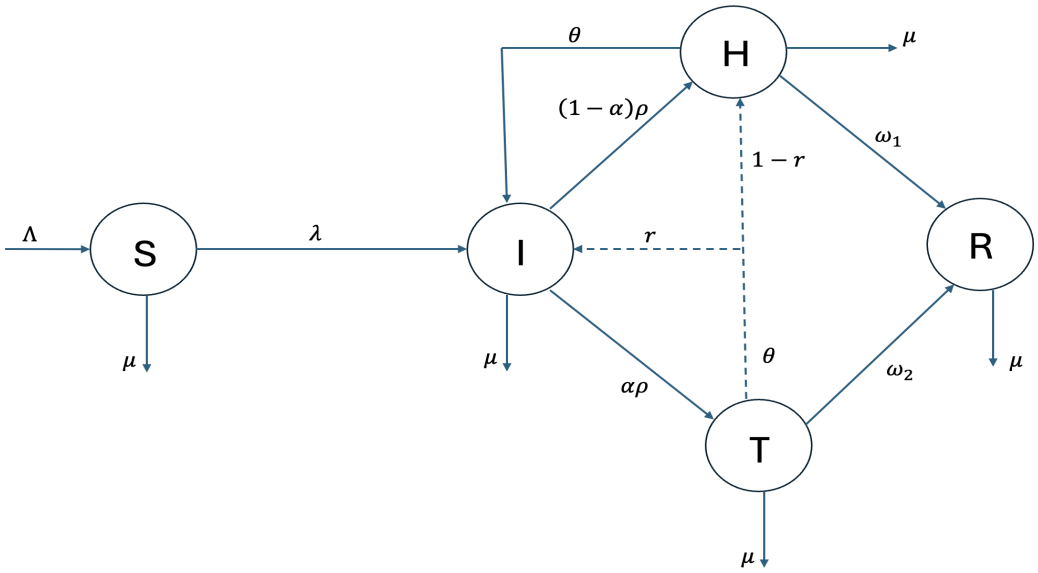

Figure 1. Model flow chart illustrating the dynamics of HCV.

Boundedness and Positivity of Solutions

Let

$$N(t) = S(t) + I(t) + H(t) + T(t) + R(t)$$

denote the total population. Summing the equations of system (1), we obtain

$$\frac{dN}{dt} = \Lambda - \mu N.$$

Solving this equation gives

$$N(t) = N(0)e^{-\mu t} + \frac{\Lambda}{\mu}(1 - e^{-\mu t}),$$

which implies that

$$\lim_{t\to\infty} N(t) = \frac{\Lambda}{\mu}.$$

Therefore, the total population is bounded and the region

$$\mathcal{G} = \left\{(S, I, H, T, R) \in \mathbb{R}^5_+ | N(t) \leq \frac{\Lambda}{\mu}\right\} \tag{2}$$

is positively invariant and attracting with respect to the model system (1).

This result is important because it ensures that the model solutions remain nonnegative and biologically feasible for $t \geq 0$, with the total population remaining finite. Thus, the region $\mathcal{G}$ provides a biologically meaningful domain for the subsequent mathematical and epidemiological analyses.

3. Model Analysis

In this section, we analyze system (1) by first determining the disease-free equilibrium (DFE). We then derive the basic reproduction number $\mathcal{R}_0$ using the next-generation matrix approach. Next, we investigate the stability of the disease-free equilibrium in terms of $\mathcal{R}_0$. Furthermore, we establish conditions for uniform persistence of the system and examine the global stability of the endemic equilibrium when $R_0 > 1$.

3.1. The Disease-Free Equilibrium and Basic Reproduction Number

System (1) has an apparent equilibrium when there is no disease, given by

$$\mathcal{E}^0 = (S_1, 0, 0, 0, 0) = \left(\frac{\Lambda}{\mu}, 0, 0, 0, 0\right) \tag{3}$$

Using the next-generation matrix approach from van den Driessche and Watmough [26], we derive the basic reproduction number $\mathcal{R}_0$ for system (1). Let F and V represent the matrices of new infection terms and transfer terms, respectively, linearized at the disease-free equilibrium $\mathcal{E}^0$. These are given by:

$$F = \begin{pmatrix} c\beta(1-\delta) & \beta(1-\delta)(1-\eta)\phi & 0 \\ 0 & 0 & 0 \\ 0 & 0 & 0 \end{pmatrix}, \quad V = \begin{pmatrix} m_1 & -\theta & -r\theta \\ -(1-\alpha)\rho & m_2 & -(1-r)\theta \\ -\alpha\rho & 0 & m_3 \end{pmatrix}, \tag{4}$$

where $m_1 = \mu + \rho$, $m_2 = \theta + \mu + \omega_1$, and $m_3 = \theta + \mu + \omega_2$. Since $\alpha, \eta, \delta, r \in [0, 1]$, it follows that $1-\alpha, \quad 1-\eta, \quad 1-\delta, \quad 1-r \geq 0$. The next-generation matrix is $K = FV^{-1}$, and the basic reproduction number is given by its spectral radius:

$$\mathcal{R}_0 = \rho(FV^{-1}) = \frac{\beta(1-\delta)[(1-r)\alpha(1-\eta)\theta\rho\phi + ((1-\alpha)(1-\eta)\rho\phi + cm_2)m_3]}{m_2(m_1m_3 - r\alpha\theta\rho) - \theta\rho[(1-r)\alpha\theta + (1-\alpha)m_3]}. \tag{5}$$

Based on this expression, we now state the following result regarding the local stability of the disease-free equilibrium.

Theorem 1. *If the basic reproduction number $\mathcal{R}_0 < 1$, then the disease-free equilibrium $\mathcal{E}^0$ is locally asymptotically stable. Conversely, if $\mathcal{R}_0 > 1$, then $\mathcal{E}^0$ is unstable.*

Proof. This result follows directly from Theorem 2 of [26], which states that the local stability of the disease-free equilibrium is determined by the spectral radius of the next-generation matrix $K = FV^{-1}$, as defined in (4).

Specifically, if $\mathcal{R}_0 = \rho(K) < 1$, then the eigenvalues of the Jacobian matrix associated with the infected subsystem all have negative real parts, implying that the DFE is locally asymptotically stable. Conversely, if $\mathcal{R}_0 > 1$, then at least one eigenvalue has a positive real part, indicating that the DFE is unstable.

Thus, the theorem is proven. □

Now to ascertain the global stability of the DFE, we employ the comparison principle with the next-generation matrix approach. The infected subsystem is compared with an appropriate linear auxiliary system, and the stability of this system is determined using the spectral radius criterion associated with the next-generation matrix. We state the following theorem,

Theorem 2. *If the basic reproduction number $\mathcal{R}_0 < 1$, then the disease-free equilibrium $\mathcal{E}^0$ of system (1) is globally asymptotically stable in the biologically feasible region $\mathcal{G}$.*

Proof. From the first equation of system (1), we have

$$\frac{dS}{dt} = \Lambda - \frac{(1-\delta)\beta(cI + \phi(1-\eta)H)S}{N} - \mu S \leq \Lambda - \mu S.$$

Applying the Gronwall inequality [27], it follows that

$$\limsup_{t\to\infty} S(t) \le \frac{\Lambda}{\mu} = S^0.$$

Also, since

$$\frac{dN}{dt} = \Lambda - \mu N,$$

we have

$$N(t) \to \frac{\Lambda}{\mu} = S^0 \qquad \text{as } t \to \infty.$$

Hence, for any sufficiently small $v > 0$ with $0 < v < S^0$, there exists $t_1 > 0$ such that for all $t \ge t_1$,

$$S(t) \le S^0 + v \qquad \text{and} \qquad N(t) \ge S^0 - v.$$

Therefore, for $t \ge t_1$,

$$\frac{S(t)}{N(t)} \le \frac{S^0 + v}{S^0 - v}.$$

Using this estimate, the infected components satisfy

$$\begin{aligned}
\frac{dI}{dt} &\le (1-\delta)\beta\frac{S^0+v}{S^0-v}\big(cI + \phi(1-\eta)H\big) + \theta(rT + H) - (\rho+\mu)I,\\
\frac{dH}{dt} &= (1-r)\theta T + (1-\alpha)\rho I - (\mu+\omega_1+\theta)H,\\
\frac{dT}{dt} &= \alpha\rho I - (\mu+\omega_2+\theta)T.
\end{aligned}$$

Consider the auxiliary linear system:

$$\begin{aligned}
\frac{dI^\star}{dt} &= (1-\delta)\beta\frac{S^0+v}{S^0-v}\big(cI^\star + \phi(1-\eta)H^\star\big) + \theta(rT^\star + H^\star) - (\rho+\mu)I^\star,\\
\frac{dH^\star}{dt} &= (1-r)\theta T^\star + (1-\alpha)\rho I^\star - (\mu+\omega_1+\theta)H^\star,\\
\frac{dT^\star}{dt} &= \alpha\rho I^\star - (\mu+\omega_2+\theta)T^\star.
\end{aligned}$$

Since the infected subsystem is cooperative, the comparison principle implies that

$$(I(t), H(t), T(t)) \le (I^\star(t), H^\star(t), T^\star(t)), \qquad \forall t \ge t_1.$$

Let

$$X^\star = \begin{pmatrix} I^\star \\ H^\star \\ T^\star \end{pmatrix}.$$

Then the auxiliary system can be written as

$$\frac{dX^\star}{dt} = (F_v - V)X^\star,$$

where

$$F_v = \begin{pmatrix} (1-\delta)\beta c\dfrac{S^0+v}{S^0-v} & (1-\delta)\beta\phi(1-\eta)\dfrac{S^0+v}{S^0-v} & 0 \\ 0 & 0 & 0 \\ 0 & 0 & 0 \end{pmatrix}, \qquad V = \begin{pmatrix} \rho+\mu & -\theta & -r\theta \\ -(1-\alpha)\rho & \mu+\omega_1+\theta & -(1-r)\theta \\ -\alpha\rho & 0 & \mu+\omega_2+\theta \end{pmatrix}.$$

At $v = 0$, we recover the matrix pair (F, V) used in the definition of $\mathcal{R}_0$, namely

$$\mathcal{R}_0 = \rho(FV^{-1}) < 1.$$

Since $\rho(F_v V^{-1})$ depends continuously on v, there exists $v_0 > 0$ such that for all $0 < v < v_0$,

$$\rho(F_v V^{-1}) < 1.$$

It follows that the Metzler matrix $F_v - V$ is Hurwitz; that is, all its eigenvalues have negative real parts. Hence,

$$(I^\star(t), H^\star(t), T^\star(t)) \to (0,0,0) \qquad \text{as } t \to \infty.$$

By comparison, we conclude that

$$(I(t), H(t), T(t)) \to (0,0,0) \qquad \text{as } t \to \infty.$$

Next, from system (1),

$$\frac{dR}{dt} = \omega_1 H + \omega_2 T - \mu R.$$

Since $H(t) \to 0$ and $T(t) \to 0$, it follows that

$$R(t) \to 0 \qquad \text{as } t \to \infty.$$

Finally, since

$$N(t) \to \frac{\Lambda}{\mu} = S^0 \qquad \text{and} \qquad S(t) = N(t) - I(t) - H(t) - T(t) - R(t),$$

we obtain

$$S(t) \to S^0 \qquad \text{as } t \to \infty.$$

Therefore,

$$(S(t), I(t), H(t), T(t), R(t)) \to (S^0, 0, 0, 0, 0) = \mathcal{E}^0,$$

which proves that $\mathcal{E}^0$ is globally asymptotically stable in $\mathcal{G}$ whenever $\mathcal{R}_0 < 1$. □

The result established in Theorem 2 highlights that $\mathcal{R}_0 = 1$ serves as a critical threshold for the disease dynamics: the disease dies out when $\mathcal{R}_0 < 1$, and persists when $\mathcal{R}_0 > 1$. From a biological standpoint, uniform persistence implies that the disease remains present in the population over a long period of time without dying out. In what follows, we formally establish the uniform persistence of the system by stating and proving the following theorem.

Theorem 3. *If $\mathcal{R}_0 > 1$, system (1) is uniformly persistent. That is, there exists a constant $\xi > 0$ such that*

$$\liminf_{t\to\infty} S(t) > \xi, \quad \liminf_{t\to\infty} I(t) > \xi, \quad \liminf_{t\to\infty} H(t) > \xi, \quad \liminf_{t\to\infty} T(t) > \xi, \quad \liminf_{t\to\infty} R(t) > \xi \tag{6}$$

with ξ being independent of initial data in $\mathcal{G}$.

Proof. Let $X = \mathcal{G}$, let the state vector be $x = (S, I, H, T, R)$, and define the positively invariant set

$$X_0 = \{x \in X \mid I + H + T + R > 0\}.$$

Then, the boundary of this set is given by

$$\partial X_0 = X \setminus X_0 = \{x \in X \mid I = H = T = R = 0\}.$$

Let ψ_t denote the semiflow induced by system (1), where $\psi_t x$ represents the state of the system at time t starting from the initial condition x, and $\psi_t X_0 = \{\psi_t x : x \in X_0\}$ denotes the set of states reached at time t from initial conditions in X_0. Moreover, $\psi_t X_0 \subset X_0$ for all $t \geq 0$.

Observe that the disease-free equilibrium (DFE) lies entirely within ∂X_0 and is the unique equilibrium in this region. Further, it is globally asymptotically stable on ∂X_0. That is,

$$\bigcup_{x \in M_\partial} \omega(x) = \{\mathcal{E}^0\},$$

where $M_\partial = \{x \in \partial X_0 \mid \psi_t x \in \partial X_0, \ \forall t \geq 0\}$ and $\omega(x)$ denotes the omega-limit set of x.

Importantly, no subset of M_∂ forms a closed orbit (cycle), and the DFE is unstable in X_0 whenever $\mathcal{R}_0 > 1$, where $\mathcal{R}_0$ is the basic reproduction number associated with system (1).

Thus, by applying Theorem 1.3.1 and Remark 1.3.1 from [28], we conclude that the system is uniformly persistent when $\mathcal{R}_0 > 1$. This completes the proof. □

3.2. Endemic Equilibrium

3.2.1. Existence of the Endemic Equilibrium

In this section, we determine the endemic equilibrium point of system (1). When $R_0 > 1$, the system admits a unique endemic equilibrium:

$$E^* = (S^*, I^*, H^*, T^*, R^*)$$

in the interior of the feasible region $\mathcal{G}$.

The endemic equilibrium can be written explicitly in terms of $\mathcal{R}_0$ as

$$S^* = \frac{\Lambda}{\mu R_0}, \ \ I^* = \frac{\Lambda m_2 m_3 (R_0 - 1)}{R_0 D}, \ \ T^* = \frac{\alpha\rho}{m_3} I^*, \ \ H^* = \frac{\rho[m_3(1-\alpha) + \alpha\theta(1-r)]}{m_2 m_3} I^*,$$

and

$$R^* = \frac{\rho[m_2\alpha\omega_1 + m_3(1-\alpha)\omega_2 + \alpha\theta(1-r)\omega_2]}{m_2 m_3 \mu} I^*,$$

where

$$m_1 = \mu + \rho, \quad m_2 = \mu + \omega_1 + \theta, \quad m_3 = \mu + \omega_2 + \theta, \quad D = m_2(m_1 m_3 - r\alpha\theta\rho) - \theta\rho[(1-r)\alpha\theta + (1-\alpha)m_3].$$

Since $I^* > 0$ if and only if $R_0 > 1$, the unique endemic equilibrium exists whenever $R_0 > 1$.

3.2.2. Global Stability of the Endemic Equilibrium

Theorem 4. *If $R_0 > 1$, the endemic equilibrium point $\mathcal{C}^* = (S^*, I^*, H^*, T^*, R^*)$ of system (1) is globally asymptotically stable in the interior of the feasible region.*

Proof. To study the global asymptotic stability of the endemic equilibrium, following [29,30], we use a Lyapunov function V as follows:

$$\begin{aligned} V \ = \ & \left(S - S^* - S^* \ln \frac{S}{S^*}\right) + V_1 \left(I - I^* - I^* \ln \frac{I}{I^*}\right) + V_2 \left(H - H^* - H^* \ln \frac{H}{H^*}\right) \\ & + V_3 \left(T - T^* - T^* \ln \frac{T}{T^*}\right) + V_4 \left(R - R^* - R^* \ln \frac{R}{R^*}\right), \end{aligned} \tag{7}$$

where $V_1, V_2, V_3, V_4 > 0$ are constants to be determined later. Applying the replacements

$$\frac{S}{S^*} = m, \quad \frac{I}{I^*} = n, \quad \frac{H}{H^*} = x, \quad \frac{T}{T^*} = y, \quad \frac{R}{R^*} = z, \tag{8}$$

the derivative of V is given by

$$\begin{aligned}
\dot{V} &= \left(1 - \frac{S^*}{S}\right)\frac{dS}{dt} + V_1\left(1 - \frac{I^*}{I}\right)\frac{dI}{dt} + V_2\left(1 - \frac{H^*}{H}\right)\frac{dH}{dt} \\
&\quad + V_3\left(1 - \frac{T^*}{T}\right)\frac{dT}{dt} + V_4\left(1 - \frac{R^*}{R}\right)\frac{dR}{dt} \\
&= \left(1 - \frac{1}{m}\right)\left[\Lambda - \frac{(1-\delta)\beta(cI + \phi(1-\eta)H)S}{N} - \mu S\right] \\
&\quad + V_1\left(1 - \frac{1}{n}\right)\left[\frac{(1-\delta)\beta(cI + \phi(1-\eta)H)S}{N} + \theta(rT + H) - (\rho + \mu)I\right] \\
&\quad + V_2\left(1 - \frac{1}{x}\right)[(1-r)\theta T + (1-\alpha)\rho I - (\mu + \omega_1 + \theta)H] \\
&\quad + V_3\left(1 - \frac{1}{y}\right)[\alpha\rho I - (\mu + \omega_2 + \theta)T] \\
&\quad + V_4\left(1 - \frac{1}{z}\right)[\omega_1 H + \omega_2 T - \mu R].
\end{aligned} \tag{9}$$

Substitute $S = mS^*$, $I = nI^*$, $H = xH^*$, $T = yT^*$, $R = zR^*$ and expand each transition rate separately. At the endemic equilibrium point, system (1) has the following identities:

$$\begin{cases}
\Lambda &= \dfrac{(1-\delta)\beta(cI^* + \phi(1-\eta)H^*)S^*}{N} + \mu S^*, \\
\dfrac{(1-\delta)\beta(cI^* + \phi(1-\eta)H^*)S^*}{N} + \theta(rT^* + H^*) &= (\rho + \mu)I^*, \\
(1-r)\theta T^* + (1-\alpha)\rho I^* &= (\mu + \omega_1 + \theta)H^*, \\
\alpha\rho I^* &= (\mu + \omega_2 + \theta)T^*, \\
\omega_1 H^* + \omega_2 T^* &= \mu R^*.
\end{cases} \tag{10}$$

After substituting these identities and collecting like terms, the linear (unpaired) deviation terms in m, n, x, y, z must have zero coefficients for $\dot{V}$ to reduce to a sum of non-positive groups. This yields the system

$$\begin{cases}
(V_1 - 1)\dfrac{(1-\delta)\beta c I^* S^*}{N} = 0, \\
(V_1 - 1)\dfrac{(1-\delta)\beta\phi(1-\eta)H^* S^*}{N} = 0, \\
(V_2 - V_1)(1-\alpha)\rho I^* = 0, \\
(V_3 - V_1)\alpha\rho I^* = 0, \\
(V_1 - V_3)r\theta T^* = 0, \\
(V_2 - V_3)(1-r)\theta T^* = 0, \\
(V_1 - V_2)\theta H^* = 0, \\
(V_4 - V_2)\omega_1 H^* = 0, \\
(V_4 - V_3)\omega_2 T^* = 0.
\end{cases} \tag{11}$$

From (11) it follows that $V_1 = V_2 = V_3 = V_4 = 1$. Thus, we now have

$$\begin{aligned}\dot{V} = &\left(1-\frac{1}{m}\right)\left[\Lambda - \lambda - \mu m S^*\right] \\ &+ \left(1-\frac{1}{n}\right)\left[\lambda + \theta(ryT^* + xH^*) - (\rho+\mu)nI^*\right] \\ &+ \left(1-\frac{1}{x}\right)\left[(1-r)\theta yT^* + (1-\alpha)\rho nI^* - (\mu+\omega_1+\theta)xH^*\right] \\ &+ \left(1-\frac{1}{y}\right)\left[\alpha\rho nI^* - (\mu+\omega_2+\theta)yT^*\right] \\ &+ \left(1-\frac{1}{z}\right)\left[\omega_1 xH^* + \omega_2 yT^* - \mu z R^*\right], \end{aligned} \tag{12}$$

where

$$\lambda = \frac{(1-\delta)\beta S^*}{N}\left(cnI^* + \phi(1-\eta)xH^*\right).$$

It then follows that

$$\begin{aligned}\dot{V} = &\mu S^*\left(1-\frac{1}{m}\right)(1-m) \\ &+ \frac{(1-\delta)\beta c I^* S^*}{N}\left[\left(1-\frac{1}{m}\right)(1-n) + \left(1-\frac{1}{n}\right)(n-m)\right] \\ &+ \frac{(1-\delta)\beta\phi(1-\eta)H^* S^*}{N}\left[\left(1-\frac{1}{m}\right)(1-x) + \left(1-\frac{1}{n}\right)(x-m)\right] \\ &+ \theta r T^*\left(1-\frac{1}{n}\right)(y-n) \\ &+ (1-r)\theta T^*\left(1-\frac{1}{x}\right)(y-x) \\ &+ \alpha\rho I^*\left(1-\frac{1}{y}\right)(n-y) \\ &+ (1-\alpha)\rho I^*\left(1-\frac{1}{x}\right)(n-x) \\ &+ \theta H^*\left(1-\frac{1}{n}\right)(x-n) \\ &+ \omega_1 H^*\left(1-\frac{1}{z}\right)(x-z) \\ &+ \omega_2 T^*\left(1-\frac{1}{z}\right)(y-z). \end{aligned} \tag{13}$$

Substituting $V_1 = V_2 = V_3 = V_4 = 1$ and simplifying yields

$$\begin{aligned}\dot{V} \;=\; &\mu S^*\left(2-m-\frac{1}{m}\right) + \frac{(1-\delta)\beta c I^* S^*}{N}\left(3-\frac{1}{m}-\frac{m}{n}-n\right) \\ &+\frac{(1-\delta)\beta\phi(1-\eta)H^* S^*}{N}\left(3-\frac{1}{m}-\frac{x}{n}-\frac{mn}{x}\right) \\ &+\theta r T^*\left(2-\frac{y}{n}-\frac{n}{y}\right) + (1-r)\theta T^*\left(2-\frac{y}{x}-\frac{x}{y}\right) \\ &+\alpha\rho I^*\left(2-\frac{n}{y}-\frac{y}{n}\right) + (1-\alpha)\rho I^*\left(2-\frac{n}{x}-\frac{x}{n}\right) \\ &+\theta H^*\left(2-\frac{x}{n}-\frac{n}{x}\right) + \omega_1 H^*\left(2-\frac{x}{z}-\frac{z}{x}\right) \end{aligned}$$

$$+\omega_2 T^* \left(2 - \frac{y}{z} - \frac{z}{y}\right). \tag{14}$$

We define the set $\mathcal{G}$ of all the above terms as

$$\mathcal{G} = \left\{m,\, n,\, x,\, y,\, z,\, \frac{1}{m},\, \frac{m}{n},\, \frac{x}{n},\, \frac{mn}{x},\, \frac{y}{n},\, \frac{n}{y},\, \frac{y}{x},\, \frac{x}{y},\, \frac{n}{x},\, \frac{y}{z},\, \frac{z}{y},\, \frac{x}{z},\, \frac{z}{x}\right\}. \tag{15}$$

Then we create subsets of $\mathcal{G}$ where the product of each subset equals one:

$$\left\{m, \frac{1}{m}\right\},\quad \left\{\frac{1}{m}, \frac{m}{n}, n\right\},\quad \left\{\frac{1}{m}, \frac{x}{n}, \frac{mn}{x}\right\},\quad \left\{\frac{y}{n}, \frac{n}{y}\right\},\quad \left\{\frac{y}{x}, \frac{x}{y}\right\},\quad \left\{\frac{n}{y}, \frac{y}{n}\right\},\quad \left\{\frac{n}{x}, \frac{x}{n}\right\},\quad \left\{\frac{y}{z}, \frac{z}{y}\right\},\quad \left\{\frac{x}{z}, \frac{z}{x}\right\}. \tag{16}$$

By the arithmetic mean–geometric mean inequality, we have:

- $2 - m - \frac{1}{m} \leq 0$ for $m > 0$, with equality if and only if $m = 1$,
- $3 - \frac{1}{m} - \frac{m}{n} - n \leq 0$ for $m, n > 0$, with equality if and only if $m = n = 1$,
- $3 - \frac{1}{m} - \frac{x}{n} - \frac{mn}{x} \leq 0$ for $m, x, n > 0$, with equality if and only if $m = x = n = 1$,
- $2 - \frac{y}{n} - \frac{n}{y} \leq 0$ for $y, n > 0$, with equality if and only if $y = n$,
- $2 - \frac{y}{x} - \frac{x}{y} \leq 0$ for $y, x > 0$, with equality if and only if $y = x$,
- $2 - \frac{n}{y} - \frac{y}{n} \leq 0$ for $n, y > 0$, with equality if and only if $n = y$,
- $2 - \frac{n}{x} - \frac{x}{n} \leq 0$ for $n, x > 0$, with equality if and only if $n = x$,
- $2 - \frac{y}{z} - \frac{z}{y} \leq 0$ for $y, z > 0$, with equality if and only if $y = z$,
- $2 - \frac{x}{z} - \frac{z}{x} \leq 0$ for $x, z > 0$, with equality if and only if $x = z$.

Since all coefficients μS^*, $\frac{(1-\delta)\beta c I^* S^*}{N}$, $\frac{(1-\delta)\beta\phi(1-\eta)H^* S^*}{N}$, $\theta r T^*$, $(1-r)\theta T^*$, $\alpha\rho I^*$, $(1-\alpha)\rho I^*$, θH^*, $\omega_1 H^*$, $\omega_2 T^*$ are strictly positive at the endemic equilibrium, each group is non-positive, and therefore $\dot{V} \leq 0$. Moreover, $\dot{V} = 0$ if and only if $m = n = x = y = z = 1$. The maximum invariant set of the system (1) on the set $\{(m, n, x, y, z) : \dot{V} = 0\}$ is the singleton $(1, 1, 1, 1, 1)$. Therefore, by LaSalle's invariance principle, the endemic equilibrium $\mathcal{C}^*$ is globally asymptotically stable whenever $R_0 > 1$. □

The global stability of the endemic equilibrium suggests that when $R_0 > 1$, HCV continues to circulate among PWID and persists at an endemic level.

4. Numerical Simulations

In this section, we present the numerical simulations to complement the analytical results and then also provide further insight into the dynamics of HCV transmission under varying epidemiological and behavioral conditions. We also seek to quantify the impact of key model parameters on the basic reproduction number $\mathcal{R}_0$ and the progression of different population compartments.

The analytical framework combines parameter-based simulations, sensitivity analysis, and scenario exploration. Table 1 summarizes the baseline parameter values used in the simulations, while Figure 2 presents a partial rank correlation coefficient (PRCC) analysis to identify the most influential parameters driving the reproduction number $\mathcal{R}_0$. Subsequent subsections then build on this foundation by systematically exploring how variations in key parameters affect disease dynamics.

Figure 2 depicts a few parameters that have an influence on the basic reproduction number $\mathcal{R}_0$, revealing the key transmission and intervention levers in the HCV model.

The transmission probability per sharing event (β) and the average number of partners for infectious individuals (c) dominate the positive correlations (PRCC $\approx +0.8$). This means that HCV persistence in the injecting population is highly sensitive to contact intensity and the efficiency of infection per sharing act. Hence, any policy that reduces either β or c, for instance, via needle and syringe programs, peer network reduction, or safe injection education produces a disproportionate decline in epidemic potential. In contrast, the treatment-seeking rate (ρ) stands out as the single strongest negative driver (PRCC ≈ -0.65), highlighting that rapid initiation of therapy and wide treatment coverage have the greatest suppressive impact on $\mathcal{R}_0$. Natural mortality (μ) and spontaneous clearance (δ) also show moderate negative effects, indicating that biological removal and immune clearance modestly help offset transmission pressure but are secondary to behavioral control and treatment uptake. Other parameters, such as relapse rates and recovery terms, display relatively weak correlations and thus contribute minimally to overall variability in $\mathcal{R}_0$. Taken together, this analysis isolates the critical control axes of the system: transmission intensity (β, c) and treatment engagement (ρ). These variables define the boundaries of epidemic persistence; reducing β and c limits the opportunity for infection, while increasing ρ accelerates the flow of individuals into treatment and recovery. As a result, targeted interventions that simultaneously depress transmission probabilities and boost treatment uptake are the most efficient pathways to drive $\mathcal{R}_0$ below unity and achieve sustainable HCV control.

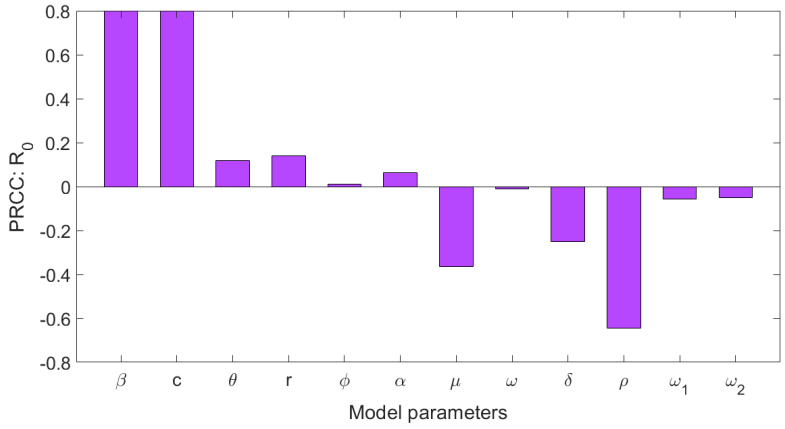

Figure 2. Partial Rank Correlation Coefficient (PRCC) analysis of model parameters with respect to the basic reproduction number ($\mathcal{R}_0$). The bars represent the magnitude and direction of the correlation between each parameter and $\mathcal{R}_0$. Positive PRCC values indicate that increasing the parameter drives $\mathcal{R}_0$ upward, like an increase, and is bad for curtailing the disease, whereas negative values denote parameters that suppress transmission potential.

Table 1. All numerical simulations were performed in Python 3.10 using the `SciPy 1.11` library. The system of ordinary differential equations in (1) was solved using `solve_ivp` with the LSODA method over a 30-year period. The initial conditions were $(S(0), I(0), H(0), T(0), R(0)) = (50{,}000, 50, 1, 0, 0)$. The parameter values used in the simulations are given in Table 1. Numerical results were visualized using `Matplotlib 3.8`. Parameters used in the HCV dynamics model among intravenous drug misusers (units = years).

Definition	Symbol	Value (Range)	Source
Recruitment rate of new intravenous drug misusers per 1000 infected	Λ	85	[31]
Natural mortality rate	μ	[0.02 (0.01–0.03)]	[32]
Probability of HCV transmission per needle-sharing event	β	[0.1 (0.084–0.1)]	[23]
Average number of needle-sharing partners for class I	c	[5 (1–10)]	[23]
Partner acquisition rate for class H	ϕ	[3 (1–10)]	[23]

Table 1. *Cont.*

Definition	Symbol	Value (Range)	Source
Reduced likelihood of HCV transmission by class H	η	[0.5 (0–1)]	Assumed
Proportion of acute infections that clear spontaneously	δ	[0.26 (0.01–0.3)]	[23,31]
Rate at which class I individuals seek treatment	ρ	[0.02 (0.01–0.03)]	[24]
Proportion of treated individuals abstaining from drug misuse	α	[0.6 (0–1)]	Assumed
Recovery rate for individuals in class H	ω_1	(0.15–0.23)	Assumed
Recovery rate for individuals in class T	ω_2	(0.15–0.23)	Assumed
Relapse rate to drug misuse for individuals in classes T and H	θ	[0.1 (0.01–0.3)]	[25]
Proportion of class T relapsing to high-risk behavior	r	[0.3 (0–0.3)]	[33]

4.1. Contour Plots of $\mathcal{R}_0$ to Assess the Effect of Parameters on the Disease Dynamics

In this subsection, we investigate the combined effects of key parameter pairs on the basic reproduction number $\mathcal{R}_0$ using contour plots.

Figure 3 presents contour plots of the basic reproduction number, $\mathcal{R}_0$, under different combinations of key parameters. In Figure 3, panel (a) shows the joint effect of the treatment-seeking rate for infectious individuals and the relapse rate of treated individuals who return to drug misuse. As expected, higher treatment-seeking rates suppress, while higher relapse rates increase it. Panel (b) is about relapse to high-risk behavior specifically, and a similar pattern emerges: reducing relapse consistently lowers transmission potential, but gains are lost if relapse rates remain high. Panel (c) highlights the combined role of recovery rates for both treated and untreated infections, with higher recovery driving below 1 and thus toward elimination thresholds. Lastly, panel (d) depicts the interplay between treatment-seeking and recovery among abstinent treated individuals, showing that strong recovery synergizes with high treatment uptake to reduce. Together, these plots emphasize that lowering relapse and improving both treatment uptake and recovery are crucial levers for reducing the epidemic potential of HCV among drug misusers.

4.2. Plots of Hypercubic Sampling of $\mathcal{R}_0$ to Assess the Impact of Parameters on the Disease Dynamics

Figure 4 presents the results of hypercubic sampling, illustrating how variability in key parameters influences the basic reproduction number $\mathcal{R}_0$. Panel (a) shows that increasing the transmission probability per needle-sharing event (β) leads to a sharp rise in $\mathcal{R}_0$, underscoring the central role of transmission efficiency. Panel (b) demonstrates a similar effect for the average number of partners (c), with larger contact networks significantly increasing $\mathcal{R}_0$. Panel (c) indicates that a higher treatment-seeking rate (ρ) suppresses $\mathcal{R}_0$, reflecting the benefit of early engagement in care. In panel (d), higher recovery rates among untreated individuals (ω_1) reduce $\mathcal{R}_0$, while panel (e) shows that improved recovery among treated individuals (ω_2) has an even stronger effect in pushing $\mathcal{R}_0$ toward values below unity. Finally, panel (f) highlights that increasing the relapse rate (θ) elevates $\mathcal{R}_0$, reversing treatment gains and sustaining transmission. Together, these results emphasize that transmission parameters (β, c) and relapse (θ) are the strongest drivers of persistence, while treatment-seeking (ρ) and recovery (ω_1, ω_2) are key levers for control.

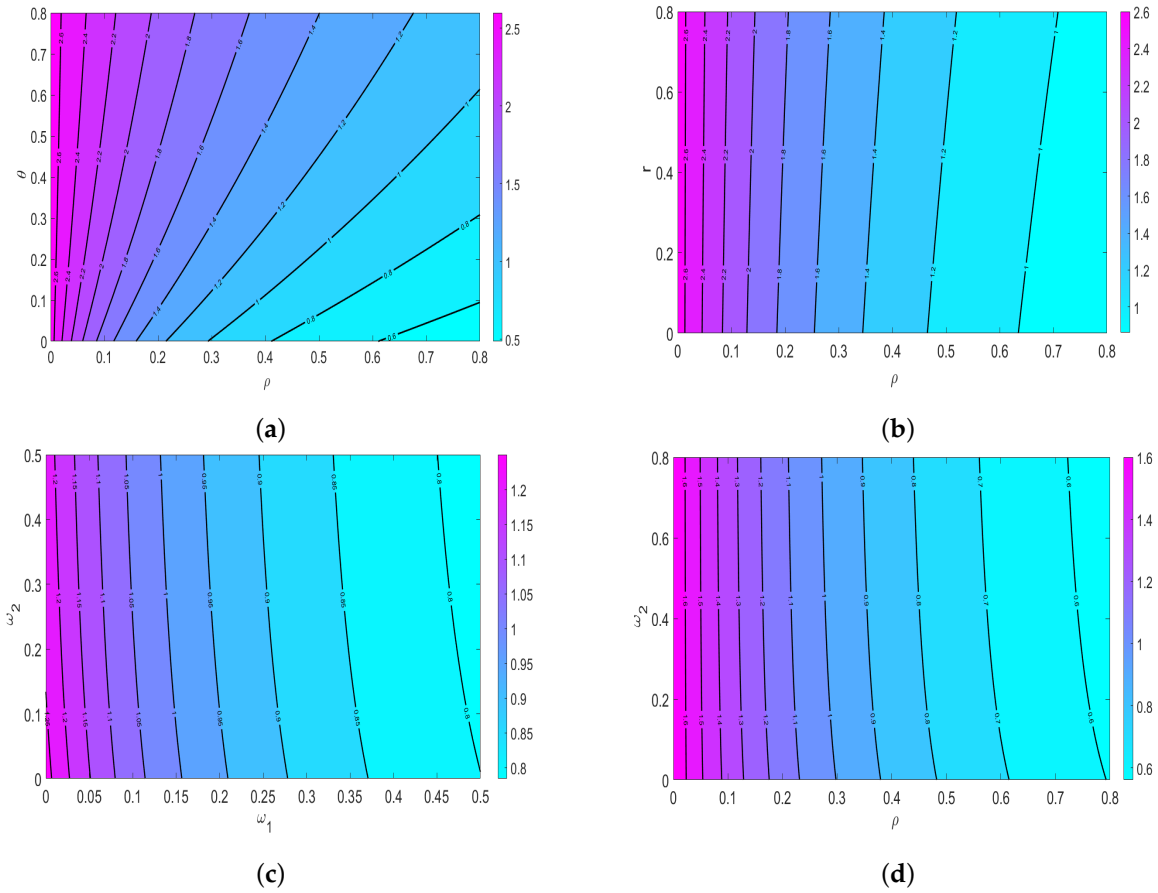

Figure 3. Contour plots of the basic reproduction number $\mathcal{R}_0$ as functions of key parameter pairs: (**a**) treatment-seeking rate for infectious individuals (ρ) and relapse rate to drug misuse for treated individuals (θ); (**b**) treatment-seeking rate (ρ) and relapse rate to high-risk behavior $(r\theta)$; (**c**) recovery rate of infected individuals not on treatment (ω_1) and on treatment (ω_2); (**d**) treatment-seeking rate (ρ) and recovery rate of abstinent treated individuals $(\alpha\omega_2)$.

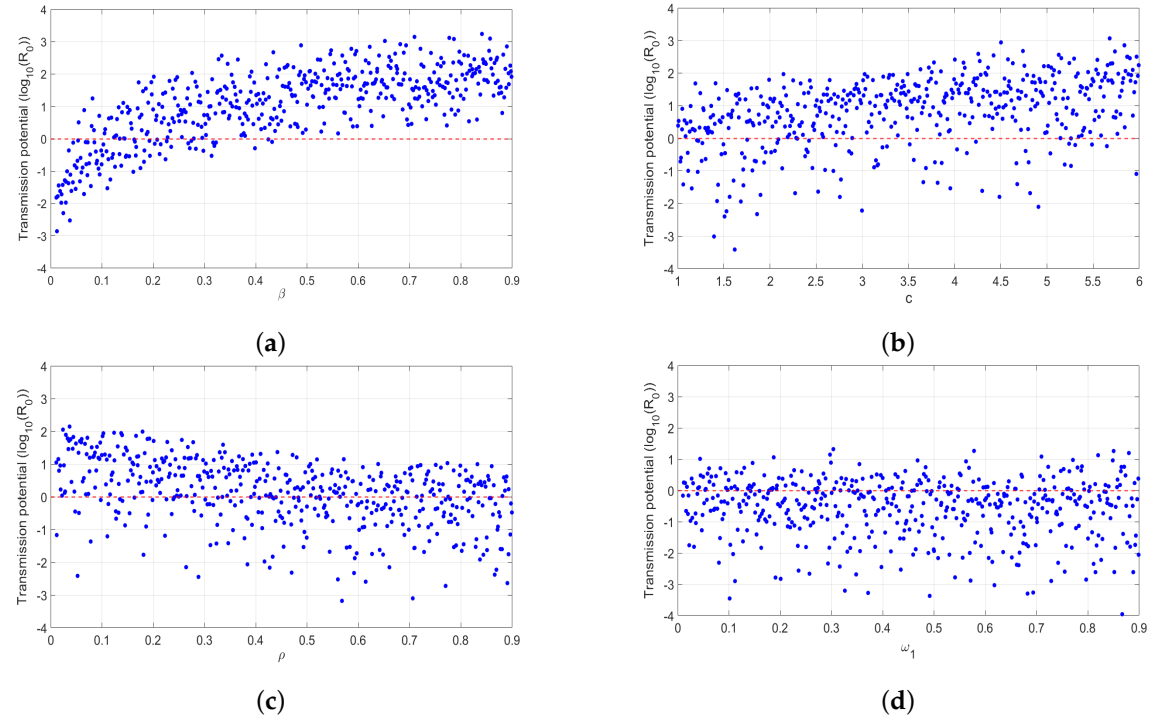

Figure 4. *Cont.*

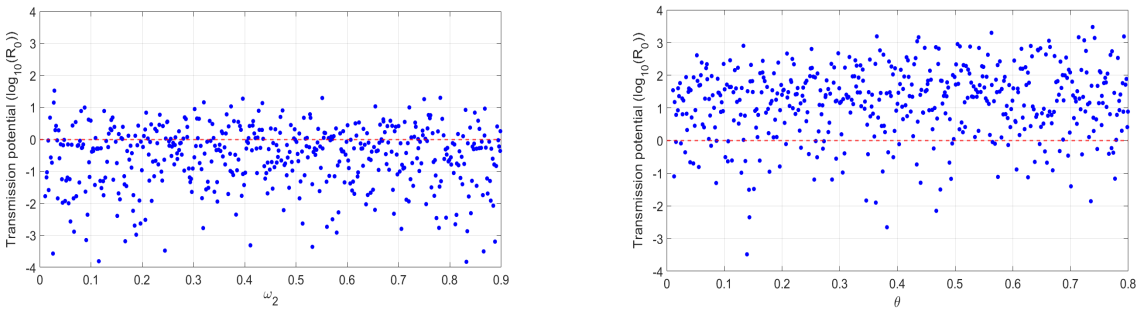

(**e**) (**f**)

Figure 4. Plots of hypercubic sampling to assess sensitivity of the basic reproduction number $\mathcal{R}_0$ to key parameters: (**a**) probability of HCV transmission per needle-sharing (β) and $\mathcal{R}_0$, (**b**) average number of needle-sharing partners for infectious individuals (c) and $\mathcal{R}_0$, (**c**) treatment-seeking rate of infected individuals (ρ) and $\mathcal{R}_0$, (**d**) recovery rate of infected individuals not on treatment (ω_1) and $\mathcal{R}_0$, (**e**) recovery rate of infected individuals on treatment (ω_2) and $\mathcal{R}_0$, (**f**) relapse rate of treated individuals returning to drug misuse (θ) and $\mathcal{R}_0$.

4.3. Effect of the Relapse Rate to Drug Misuse Among Individuals on Treatment on HCV Transmission

In this subsection, we investigate the impact of relapse to drug misuse among treated individuals on the dynamics of HCV transmission. We seek to quantify how relapse alters the distribution of individuals across epidemiological compartments and undermines treatment effectiveness.

In Figure 5a, the number of untreated infectious individuals $I(t)$ increases during the first 12 years for all values of θ and then begins to decline gradually. Higher values of θ result in slightly higher peaks but lower long-term levels of $I(t)$ after year 12. In Figure 5b,c, both the treated reduced-risk individuals $H(t)$ and the treated abstinent individuals $T(t)$ increase up to around 20 years before declining slowly; higher relapse rates lead to lower long-term populations in $H(t)$ and $T(t)$. In Figure 5d, the recovered individuals $R(t)$ show a steady increase throughout the 30-year period, although higher relapse rates result in modestly lower final levels of $R(t)$. Overall, higher relapse rates from treatment lead to larger long-term infectious populations. This shows that relapse undermines the benefits of antiviral therapy by replenishing the pool of infectious individuals.

4.4. Effect of Spontaneous Clearance on HCV Disease Transmission

This subsection focuses on the role of spontaneous viral clearance in shaping HCV transmission dynamics. Specifically, we assess how variations in the clearance parameter influence infection prevalence and recovery patterns within the population.

Figure 6 illustrates the effect of the spontaneous clearance parameter (δ) on the disease dynamics. In Figure 6a, the number of untreated infectious individuals $I(t)$ increases and peaks around year 12 for all values of δ. Higher values of δ result in a modestly lower peak and slightly faster decline after year 12. In Figure 6b–d, the treated reduced-risk individuals $H(t)$, the treated abstinent individuals $T(t)$, and the recovered individuals $R(t)$ all show a general reduction as δ increases. After the peak period (beyond year 12), increasing δ consistently lowers the levels across the infectious and treated compartments while supporting a modest increase in the recovered class $R(t)$. Thus, higher spontaneous clearance reduces the peak and long-term burden of HCV infection across most compartments, although its effect is relatively modest (varied) compared to treatment-related and behavioral parameters. This indicates that while natural clearance provides some benefit, interventions targeting treatment uptake and adherence are likely to have a stronger impact on controlling transmission among people who inject drugs.

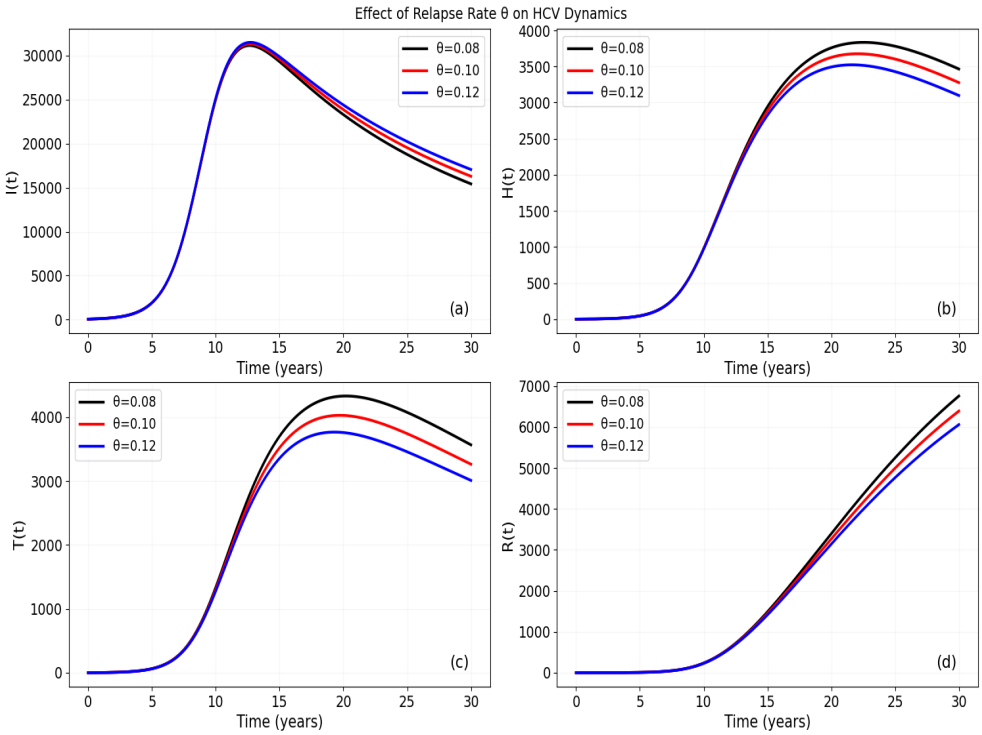

Figure 5. Numerical simulation of system (1) to investigate the effects of the relapse rate to drug misuse among treated individuals: (**a**) infected individuals not on treatment, (**b**) infected individuals who are on treatment but have reduced their number of needle-sharing partners, (**c**) infectious individuals on treatment who have abstained from drug misuse activities, and (**d**) recovered individuals from drug misuse.

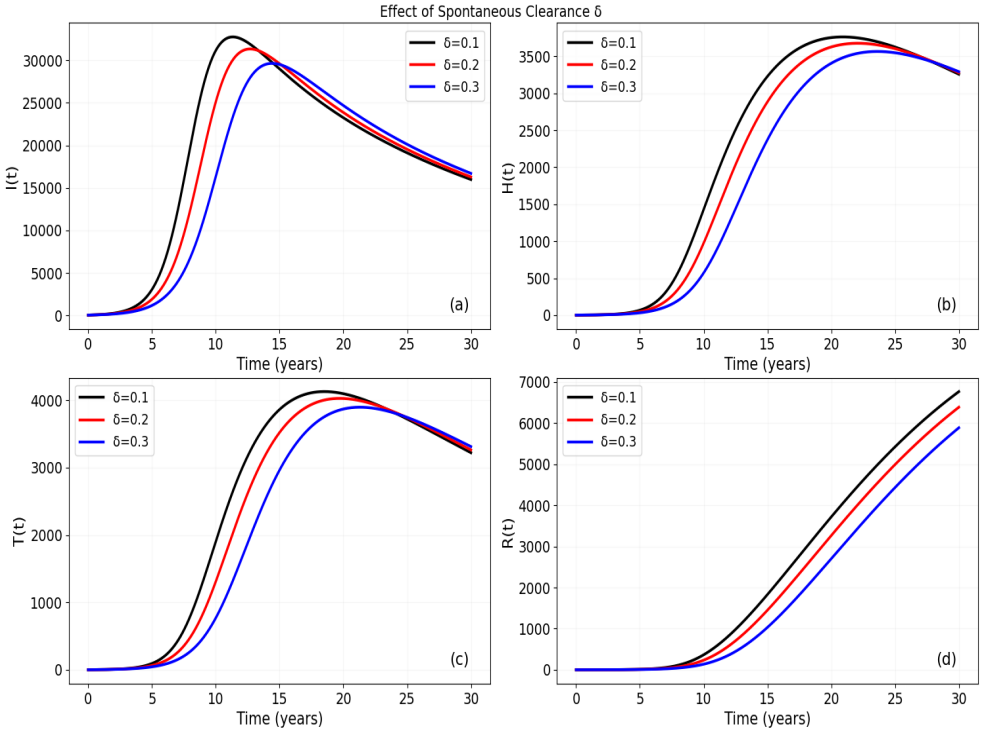

Figure 6. Numerical simulation of system (1) to investigate the impact of the spontaneous clearance rate (δ) on HCV transmission: (**a**) dynamics of infected individuals not on treatment (I), (**b**) infected individuals on treatment with reduced needle-sharing partners (H), (**c**) infectious individuals on treatment who have abstained from drug misuse activities (T), and (**d**) recovered individuals from drug misuse (R).

4.5. Impact of Treatment Adherence on HCV Transmission

Here, we examine the impact of treatment adherence, represented by the proportion of individuals who abstain from drug misuse during treatment. The objective is to evaluate how adherence influences infection control and long-term disease outcomes.

In Figure 7a, the number of untreated infectious individuals $I(t)$ shows almost no visible difference across the three values of α, indicating that treatment adherence has a negligible direct effect on the untreated infectious class. In Figure 7b, the treated reduced-risk individuals $H(t)$ decrease noticeably as α increases. In Figure 7c, the treated abstinent individuals $T(t)$ increase significantly with higher α, particularly after the first 6–8 years. In Figure 7d, the recovered individuals $R(t)$ show only minor differences across the values of α. Overall, increasing treatment adherence α has little impact on the untreated infectious class $I(t)$ but produces a clear shift from the reduced-risk treated class $H(t)$ to the abstinent treated class $T(t)$. This demonstrates that higher adherence improves the quality of treatment outcomes by directing more individuals into successful abstinence, even if the overall reduction in the infectious population appears low.

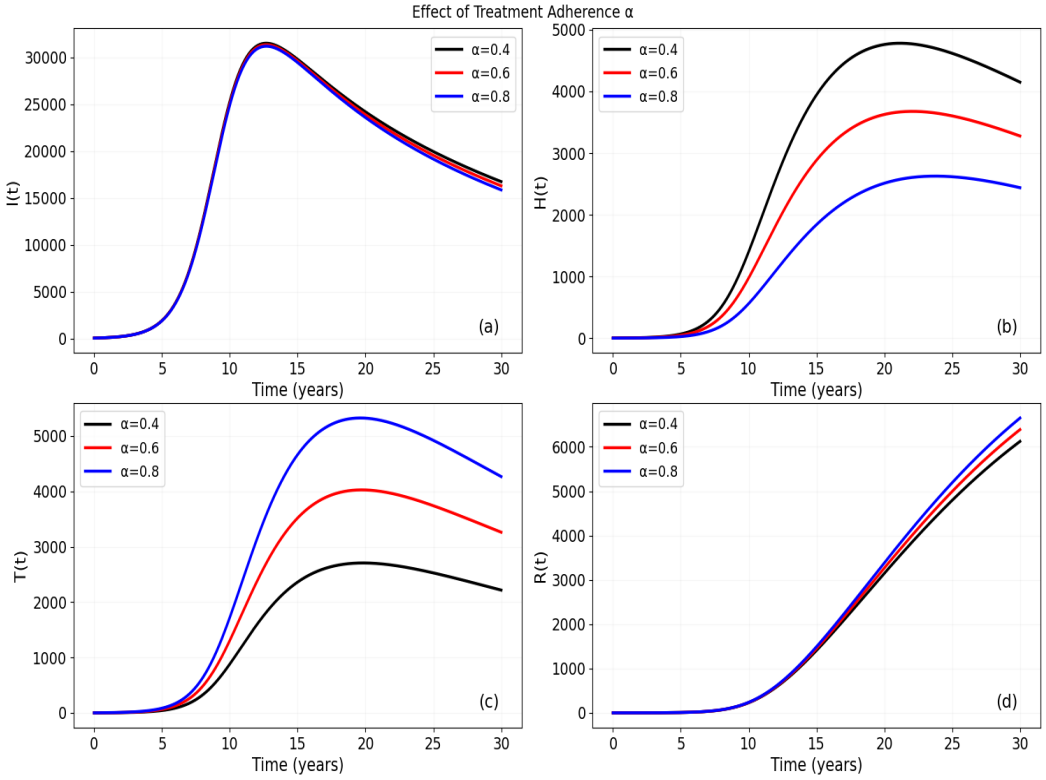

Figure 7. Numerical simulation of system (1) illustrating the effect of varying the proportion of treated individuals who abstain from drug misuse (α) on: (**a**) infectious individuals not on treatment $I(t)$; (**b**) infectious individuals on treatment who have reduced needle-sharing $H(t)$; (**c**) infectious individuals on treatment who have abstained $T(t)$; and (**d**) recovered individuals $R(t)$.

4.6. Impact of Relapse to High-Risk Behavior on HCV Transmission

This subsection explores the effect of relapse to high-risk behavior among previously abstinent individuals. It is meant to understand how behavioral reversals affect epidemic persistence and the effectiveness of treatment interventions.

In Figure 8a, the number of untreated infectious individuals $I(t)$ shows almost no visible difference across the three values of r. In Figure 8b, the treated reduced-risk individuals $H(t)$ show only minor differences until after approximately 12 years, after which higher values of r produce a noticeable increase in $H(t)$, as r is decreased. In Figure 8c,d, the

treated abstinent individuals $T(t)$ and the recovered individuals $R(t)$ remain largely unaffected by changes in r, with the curves staying very close throughout the 30-year period. Thus, varying the relapse proportion r has relatively little impact on the overall dynamics of the model. The parameter mainly affects the treated reduced-risk class $H(t)$ after the first 12 years. This suggests that while relapse influences post-treatment behavior distribution, its net effect on the broader HCV epidemic is limited under the current model assumptions.

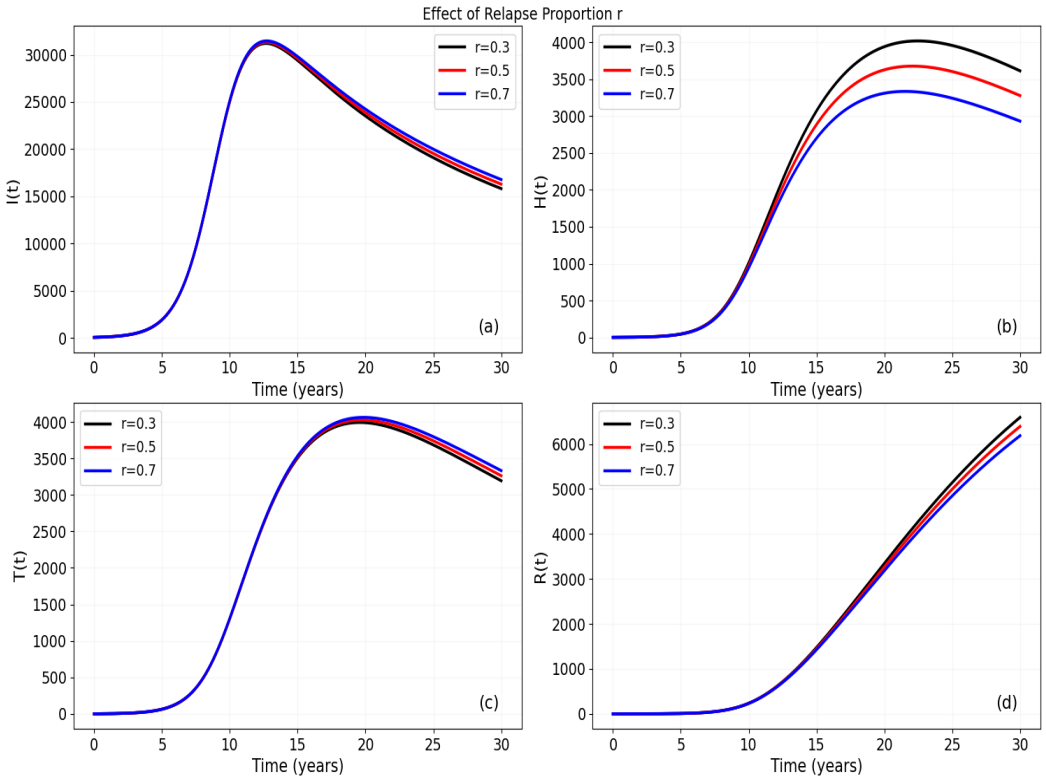

Figure 8. Numerical simulation of system (1) illustrating the effect of the relapse proportion r of abstinent individuals returning to high-risk behavior on: (**a**) infectious individuals not on treatment $I(t)$; (**b**) infectious individuals on treatment with reduced needle-sharing $H(t)$; (**c**) recovered individuals $R(t)$; and (**d**) susceptible individuals $S(t)$.

4.7. Effect of Varying the Number of Needle-Sharing Partners on HCV Transmission

In this subsection, we analyze the effect of needle-sharing behavior on HCV transmission dynamics. The objective is to try to understand how variations in contact rates influence infection spread and recovery within the population.

Figure 9 illustrates the effect of varying the number of needle-sharing partners on the epidemic dynamics of HCV. In Figure 9a, the number of untreated infectious individuals $I(t)$ increases much faster and reaches a substantially higher peak as c increases. In Figure 9b, the treated reduced-risk individuals $H(t)$ also rise significantly with higher values of c. This is also the same phenomenon observed in Figure 9c,d. Overall, varying the average number of needle-sharing partners c has the strongest impact on HCV transmission among the parameters examined. Higher contact rates lead to faster epidemic growth and substantially larger long-term infectious populations, while lower values of c markedly reduce the number of cases. This finding is consistent with the PRCC analysis in Figure 2 and confirms that reducing needle-sharing contacts is one of the most effective strategies for lowering HCV burden among people who inject drugs.

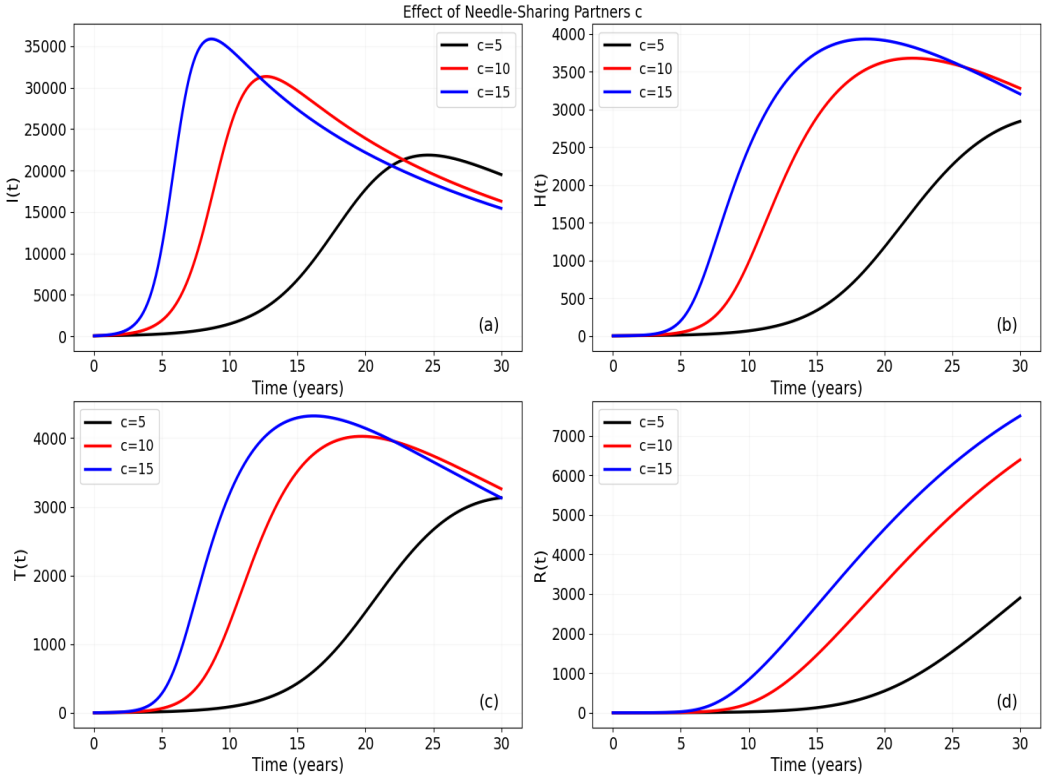

Figure 9. Numerical solution of the system (1) showing the impact of needle-sharing on: (**a**) infectious individuals (I), (**b**) treated individuals with reduced needle-sharing partners (H), (**c**) susceptible individuals (S), and (**d**) recovered individuals (R).

4.8. Effects of the Rate of Seeking Treatment on HCV Disease Transmission in Humans

Figure 10 examines the impact of treatment on infected individuals through variations in treatment engagement. Panel (a) shows the dynamics of infected individuals, illustrating a reduction in infection levels as treatment is applied. Panel (b) presents infected individuals who are on treatment and have reduced their number of needle-sharing partners, indicating that treatment uptake shifts individuals into lower-risk states. Panel (c) depicts infectious individuals on treatment who have abstained from drug misuse activities, showing improved control of infection under sustained behavioral change. Panel (d) shows recovered individuals, whose population increases as treatment effectiveness improves. Figure 10 therefore suggests the importance of treatment uptake in suppressing infection prevalence while demonstrating that sustained behavioral change is important for maximizing the long-term benefits of treatment.

In Figure 10a, the number of untreated infectious individuals $I(t)$ increases initially for all values of ρ and then begins to drop after around 12 years. Higher treatment-seeking rates lead to lower peaks and a significantly faster decline in $I(t)$. In Figure 10b–d, the treated reduced-risk individuals $H(t)$, the treated abstinent individuals $T(t)$, and the recovered individuals $R(t)$ all increase more rapidly and reach higher levels as ρ increases. Overall, increasing the treatment-seeking rate ρ substantially reduces the number of untreated infectious individuals while increasing the sizes of the treated (H and T) and recovered (R) populations, as expected. This demonstrates that higher treatment uptake is highly effective in lowering the overall HCV burden and accelerating recovery in the population of people who inject drugs.

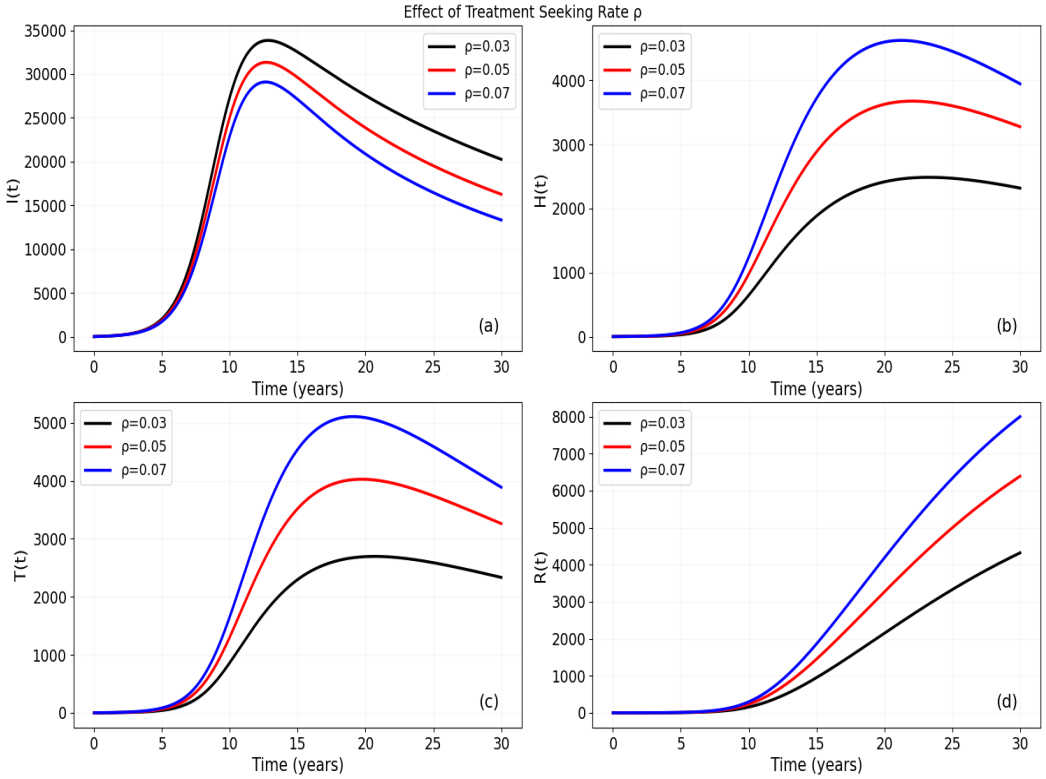

Figure 10. Simulation of system (1) to investigate the effects of treatment on infected individuals: (**a**) Numerical solution of infected individuals (**b**) infected individuals who are on treatment but have reduced their number of needle-sharing partners, (**c**) infectious individuals on treatment who have abstained from drug misuse activities, and (**d**) recovered individuals from drug misuse.

5. Discussion

Hepatitis C virus (HCV) transmission among people who inject drugs remains a major public health challenge, despite the availability of highly effective antiviral therapies. In this study, we developed and analyzed a mathematical model that incorporated treatment adherence, behavioral modification, and relapse dynamics to examine how these factors shaped HCV transmission and persistence in injecting populations. We derived the model's basic reproduction number, R_0, a threshold parameter governing long-term disease dynamics. Analytical results showed that when $R_0 < 1$, the disease-free equilibrium was globally asymptotically stable, ensuring eventual elimination of HCV regardless of initial conditions. Conversely, when $R_0 > 1$, the model exhibited uniform persistence and convergence to a unique endemic equilibrium. Sensitivity analyses and numerical simulations identified transmission intensity—captured by the probability of infection per needle-sharing event and the average number of sharing partners—as the dominant drivers of epidemic persistence. These parameters exerted the strongest positive influence on R_0, highlighting the outsized role of contact structure and risk behavior in sustaining transmission. This result supported the epidemiological importance of harm reduction interventions such as needle and syringe programs, peer network reduction, and safe injection education. Reductions in either transmission probability or contact rates produced disproportionately large decreases in epidemic potential, highlighting these interventions as critical complements to antiviral treatment. Treatment-related parameters, particularly the rate at which infected individuals initiated therapy, emerged as the strongest negative drivers of R_0. Increasing treatment uptake accelerated the removal of infectious individuals from the high-risk pool and suppressed transmission. However, the model also demonstrated that the benefits of treatment were highly contingent on adherence and sustained behavior change. Individuals who

initiated treatment but failed to abstain from drug misuse, or who relapsed after temporary abstinence, continued to contribute to transmission, albeit at reduced rates. This behavioral heterogeneity weakened the population-level impact of treatment scale-up and helped explain why real-world outcomes often fell short of elimination targets based solely on treatment coverage.

Numerical simulations identified the average number of needle-sharing partners (c) and the treatment-seeking rate (ρ) as the two parameters with the greatest influence on HCV transmission dynamics. The strong impact of c arises because higher needle-sharing frequency directly amplifies the force of infection, accelerating both the initial epidemic takeoff and the establishment of a large endemic infectious pool. This underscores why behavioral risk reduction remains fundamental. Each additional sharing partner significantly increases transmission opportunities in a high-risk network. On the other hand, ρ exerts powerful control because prompt treatment initiation rapidly removes individuals from the untreated infectious class and channels them into treated compartments, thereby reducing the duration of high infectiousness. These findings have important policy implications. Interventions aimed at lowering c, such as expanded needle and syringe programs, supervised consumption sites, and peer-led education, should be prioritized alongside aggressive scale-up of testing and immediate treatment access to increase ρ. Combining these two strategies offers the highest potential for reducing incidence and moving toward HCV elimination among people who inject drugs.

Despite its strengths, the model had limitations that warranted consideration. The assumption of homogeneous mixing might oversimplify the complex network structures that characterize injecting drug user populations, where clustering, assortative mixing, and partnership concurrency could substantially influence transmission dynamics. Additionally, the model did not explicitly account for reinfection after recovery, which might be relevant in settings with ongoing high-risk behavior. Incorporating network-based contact structures, reinfection pathways, and spatial heterogeneity would be valuable extensions of this work.

Future studies could extend the model by incorporating heterogeneity in treatment adherence and relapse behavior, as well as fitting the model to longitudinal epidemiological data to further evaluate the impact of these factors on HCV transmission among PWID.

In conclusion, this study demonstrated that effective control of HCV among people who inject drugs required more than widespread availability of antiviral therapy. Sustained reductions in transmission depended critically on treatment adherence, relapse prevention, and behavioral risk reduction. Mathematical modeling that explicitly integrated these processes provided essential insight into the mechanisms driving epidemic persistence and highlighted the need for integrated intervention strategies. By combining treatment scale-up with harm reduction and behavioral support programs, public health efforts could more effectively push the reproduction number below unity and move closer to the goal of HCV elimination in high-risk populations.

Author Contributions: Conceptualization, T.V.M. and A.M.; methodology, M.H., S.T.M., and M.Z.; software, T.V.M.; validation, M.H., T.V.M., S.T.M., and M.Z.; formal analysis, M.H., T.V.M., S.T.M., and M.Z.; investigation, T.V.M., S.T.M., M.Z., and A.M.; resources, A.M.; data curation, M.H.; writing—original draft preparation, M.H.; writing—review and editing, M.H., T.V.M., S.T.M., M.Z., and A.M.; visualization, M.H. and T.V.M.; supervision, A.M.; project administration, A.M.; funding acquisition, A.M. All authors have read and agreed to the published version of the manuscript.

Funding: This research received no external funding.

Data Availability Statement: The original contributions presented in this study are included in the article. Further inquiries can be directed to the corresponding authors.

Conflicts of Interest: The authors declare no conflicts of interest.

References

1. Smith, D.B.; Mellor, J.; Jarvis, L.M.; Davidson, F.; Kolberg, J.; Urdea, M.; Yap, P.L.; Simmonds, P. Variation of the hepatitis C virus 5′ non-coding region: Implications for secondary structure, virus detection and typing. *J. Gen. Virol.* **1995**, *76*, 1749–1761. [CrossRef] [PubMed]
2. Lavanchy, D. The global burden of hepatitis C. *Liver Int.* **2009**, *29*, 74–81. [CrossRef] [PubMed]
3. Alter, M.J. Epidemiology of hepatitis C virus infection. *World J. Gastroenterol.* **2007**, *13*, 2436–2441. [CrossRef] [PubMed]
4. Armstrong, G.L.; Wasley, A.; Simard, E.P.; McQuillan, G.M.; Kuhnert, W.L.; Alter, M.J. The prevalence of hepatitis C virus infection in the United States, 1999–2002. *Ann. Intern. Med.* **2006**, *144*, 705–714. [CrossRef] [PubMed]
5. Kim, W.R. The burden of hepatitis C in the United States. *Hepatology* **2002**, *36*, S30–S34. [CrossRef] [PubMed]
6. World Health Organization. Global Hepatitis Report 2022. Available online: https://www.who.int/news-room/fact-sheets/detail/hepatitis-c (accessed on 14 January 2024).
7. Schillie, S.; Wester, C.; Osborne, M.; Wesolowski, L. CDC recommendations for hepatitis C screening among adults. *MMWR Recomm. Rep.* **2020**, *69*, 1–17. [CrossRef] [PubMed]
8. Karimi, S.E.; Bayani, A.; Higgs, P.; Bayat, A.H.; Hemmat, M.; Ahounbar, E.; Armoon, B.; Fakhri, Y. Prevalence and high-risk behaviours associated with HCV testing among people who inject drugs: A systematic review and meta-analysis. *Subst. Abus. Treat. Prev. Policy* **2020**, *15*, 64. [CrossRef] [PubMed]
9. Simon, C.M. The SIR dynamic model of infectious disease transmission and its analogy with chemical kinetics. *PeerJ Phys. Chem.* **2020**, *2*, e14. [CrossRef]
10. Shepard, C.W.; Finelli, L.; Alter, M.J. Global epidemiology of hepatitis C virus infection. *Lancet Infect. Dis.* **2005**, *5*, 558–567. [CrossRef] [PubMed]
11. Degenhardt, L.; Peacock, A.; Colledge, S.; Leung, J.; Grebely, J.; Vickerman, P.; Larney, S.; Hickman, M.; Stone, J.; Trickey, A.; et al. Global prevalence of injecting drug use and sociodemographic characteristics and prevalence of HIV, HBV, and HCV in people who inject drugs: A multistage systematic review. *Lancet Glob. Health* **2017**, *5*, e1192–e1207. [CrossRef] [PubMed]
12. Butt, F.; Shahid, M.; Hassan, M.; Tawakkal, F.; Amin, I.; Afzal, S.; Bhatti, R.; Nawaz, R.; Idrees, M. A review on hepatitis C virus: Role of viral and host-cellular factors in replication and existing therapeutic strategies. *Egypt. Liver J.* **2022**, *12*, 71. [CrossRef]
13. Peng, L.; Xie, P.; Tang, Z.; Liu, F. Modeling and analyzing transmission of infectious diseases using generalized stochastic Petri nets. *Appl. Sci.* **2021**, *11*, 8400. [CrossRef]
14. Chen, D. Modeling the spread of infectious diseases: A review. In *Analyzing and Modeling Spatial and Temporal Dynamics of Infectious Diseases*; Jones Wiley: Hoboken, NJ, USA, 2015; pp. 19–42.
15. Buchwald, A.G.; Adams, J.; Bortz, D.M.; Carlton, E.J. Infectious disease transmission models to predict, evaluate, and improve understanding of COVID-19 trajectory and interventions. *Ann. Am. Thorac. Soc.* **2020**, *17*, 1204–1206. [CrossRef] [PubMed]
16. Greenhalgh, D.; Al-Rashidi, N. Modeling the spread of hepatitis C virus amongst people who inject drugs. *Eng. Rep.* **2022**, *4*, e12503. [CrossRef]
17. Pitcher, A.B.; Borquez, A.; Skaathun, B.; Martin, N.K. Mathematical modeling of hepatitis C virus (HCV) prevention among people who inject drugs: A review of the literature and insights for elimination strategies. *J. Theor. Biol.* **2019**, *481*, 194–201. [CrossRef] [PubMed]
18. Fang, K.; Wang, H.L.; Lin, Y.; Li, S.; Wu, J. Modeling the impacts of prevention and treatment interventions on hepatitis C among people who inject drugs in China. *Infect. Dis. Ther.* **2023**, *12*, 1043–1055. [CrossRef] [PubMed]
19. Mushanyu, J.; Chukwu, C.W. Modeling the co-dynamics of alcohol abuse and HCV transmission with integrated intervention strategies. *Math. Open* **2026**, *5*, 2650005. [CrossRef]
20. Mupedza, T.V.; Mhlanga, L.; Mamutse, D.; Helikumi, M.; Lolika, P.O.; Murambiwa, S.T.; Mhlanga, A. Modeling the effects of treatment adherence challenges on the transmission dynamics of hepatitis C virus. *PLoS ONE* **2025**, *20*, e0329543. [CrossRef] [PubMed]
21. Helikumi, M.; Mushanyu, J.; Mhlanga, A. A mathematical model of HCV transmission dynamics with sex stratification and environmental effects. *PLoS ONE* **2025**, *20*, e0336374. [CrossRef] [PubMed]
22. Mushayabasa, S. On the role of optimal counseling and antiviral therapy on controlling HCV among intravenous drug misusers. *J. Comput. Med.* **2014**, *2014*, 347827. [CrossRef]
23. Bhunu, C.P.; Mushayabasa, S. Assessing the effects of intravenous drug use on Hepatitis C transmission dynamics. *J. Biol. Syst.* **2011**, *19*, 447–460. [CrossRef]
24. Mushayabasa, S.; Bhunu, C.P. Epidemiological consequences of non-compliance to HCV therapy among IDUs. *Int. J. Res. Rev. Appl. Sci.* **2011**, *8*, 288–295.
25. Mushayabasa, S.; Bhunu, C.P. Mathematical analysis of hepatitis C model for intravenous drug misusers: Impact of antiviral therapy, abstinence and relapse. *Simulation* **2014**, *90*, 487–500. [CrossRef]

26. Van den Driessche, P.; Watmough, J. Reproduction numbers and sub-threshold endemic equilibria for compartmental models of disease transmission. *Math. Biosci.* **2002**, *180*, 29–48. [CrossRef] [PubMed]
27. Willett, D. A linear generalization of Grönwall's inequality. *Proc. Am. Math. Soc.* **1965**, *16*, 774–778. [CrossRef]
28. Zhao, X.Q. Uniform persistence and periodic coexistence states in infinite-dimensional periodic semi flows with applications. *Can. Appl. Math. Q.* **1995**, *3*, 473–495.
29. Li, J.; Yang, Y.; Zhou, Y. Global stability of an epidemic model with latent stage and vaccination. *Nonlinear Anal. Real World Appl.* **2011**, *12*, 2163–2173. [CrossRef]
30. Huo, H.-F.; Chen, R. Stability of an HIV/AIDS treatment model with different stages. *Discret. Dyn. Nat. Soc.* **2015**, *2015*, 630503. [CrossRef]
31. Martin, N.K.; Vickerman, P.; Hickman, M. Mathematical modelling of hepatitis C treatment for injecting drug users. *J. Theor. Biol.* **2011**, *274*, 58–66. [CrossRef] [PubMed]
32. Mushayabasa, S.; Bhunu, C.P.; Smith, R.J. Assessing the impact of educational campaigns on controlling HCV among women prisoners. *Commun. Nonlinear Sci. Numer. Simul.* **2012**, *17*, 1714–1724. [CrossRef]
33. Edlin, B.R. Prevention and treatment of hepatitis C in injection drug users. *Hepatology* **2002**, *36*, S210–S219. [CrossRef] [PubMed]

Disclaimer/Publisher's Note: The statements, opinions and data contained in all publications are solely those of the individual author(s) and contributor(s) and not of MDPI and/or the editor(s). MDPI and/or the editor(s) disclaim responsibility for any injury to people or property resulting from any ideas, methods, instructions or products referred to in the content.